Critical linear thermal expansion in the smectic-*A* phase near the nematic-smectic phase transition

E. Anesta and G. S. Iannacchione*
Department of Physics, Worcester Polytechnic Institute, Worcester, Massachusetts 01609, USA

C. W. Garland†
Department of Chemistry, Massachusetts Institute of Technology, Cambridge, Massachusetts 02139, USA
(Received 20 May 2004; published 21 October 2004)

Recent high-resolution x-ray investigations of the smectic-*A* (SmA) phase near the nematic-to-SmA transition provide information about the critical behavior of the linear thermal expansion coefficient $\alpha_{\parallel}$ parallel to the director. Combining such data with available volume thermal expansion α_V data yields the in-plane linear expansion coefficient $\alpha_{\perp}$. The critical behaviors of $\alpha_{\parallel}$ and $\alpha_{\perp}$ are the same as those for α_V and the heat capacity C_p. However, for any given liquid crystal, $\alpha_{\parallel}$(crit) and $\alpha_{\perp}$(crit) differ in sign. Furthermore, the quantity $\alpha_{\parallel}$(crit) is positive for SmA_d partial bilayer smectics, while it is negative for nonpolar SmA_m monomeric smectics. This feature is discussed in terms of the molecular structural aspects of these smectic phases.

DOI: 10.1103/PhysRevE.70.041703 PACS number(s): 61.30.Cz, 64.60.Fr, 64.70.Md

I. INTRODUCTION

The character of the liquid-crystal nematic (N)-smectic-A (SmA) phase transition is one of the more challenging problems in condensed-matter theory [1,2]. Detailed studies of the critical behavior show a crossover from Gaussian tricritical to *XY*-like second order as the width of the nematic range increases (i.e., the McMillan parameter $R_M \equiv T_{NA}/T_{IN}$ decreases) [2,3]. Due to Landau-Peierls instabilities, the SmA phase has a lower critical dimensionality of 3, and thus algebraic decay of smectic correlations is observed in the SmA phase [4] rather than true long-range order. Nevertheless, on length scales important for many properties, the N-SmA transition in a liquid crystal (LC) with a small R_M value behaves very much like a three-dimensional (3D) *XY* system. Detailed analyses have been made of the N-SmA critical behavior for systems in the tricritical (small N-range [5]) and 3D *XY* (large-N range [6]) limits.

The most extensive studies of the N-SmA critical behavior have been carried out in the N phase, and those measurements made in the SmA phase are mostly thermal. Heat capacity [2,3] and volume thermal expansion [7,8] data exist in both the N and SmA phases, and both of these properties show that scaling holds with $\alpha^+ = \alpha^- = \alpha$ for the critical exponent above T_{NA} and below. The layer compressional elastic constant $B(T)$ has also been studied in the SmA phase, but its critical behavior is still imperfectly understood [2,9].

Quite recently, detailed x-ray studies of the SmA region have been carried out in connection with randomly perturbed liquid crystal-aerosil dispersions; see Ref. [10] for an overall analysis of one such LC+aerosil system. X-ray studies of some pure bulk LC's and several LC-aerosil dispersions provide detailed data on the temperature dependence of the smectic layer thickness $d(T)$. Thus, such x-ray data yield the critical behavior in the SmA phase of the *linear* thermal expansion coefficient $\alpha_{\parallel}(T)$ normal to the layer (i.e., parallel to the director). Combining x-ray $\alpha_{\parallel}$ values with dilatometric data for the volume thermal expansion coefficient $\alpha_V(T)$ allows one to determine also $\alpha_{\perp}(T)$, the in-plane linear thermal expansion coefficient.

It will be shown in this paper that both the linear expansion coefficients $\alpha_{\parallel}$ and $\alpha_{\perp}$ exhibit the same critical behavior as α_V and C_p. However, $\alpha_{\parallel}$(crit) and $\alpha_{\perp}$(crit) are observed to differ in sign. Thus consideration of the behavior of the linear coefficients sheds new light on a "structural" aspect of SmA formation. The LC systems analyzed here include two partial bilayer smectics SmA_d (8CB=octylcyanobiphenyl and 8OCB=octyloxycyanobiphenyl) and three nonpolar "monomeric" smectics [11] SmA_m ($\overline{8}S5$=pentylphenylthiol octyloxybenzoate, $\overline{10}S5$ = the decyl homolog of $\overline{8}S5$, and 4O.8=butoxybenzylidene octylaniline). Table I lists the value of the critical heat capacity exponent α and the phase sequence with transition temperatures for these five LC's. The structural formulas for these molecules are shown in Fig. 1.

II. DATA ANALYSIS

In recent years, high-resolution dilatometry has yielded excellent $V(T)$ data and thus volume thermal expansion coefficients $\alpha_V(T)$ in both the N and SmA phases of several LC's [7,8,13,14]. These results, which provide much better $V(T)$ data than that obtained with Paar-type vibrating tube instruments [15], are especially good for 8CB, 8OCB, $\overline{8}S5$, and $\overline{10}S5$ [7,8]. For all four of these LC's, the analysis of the critical behavior of $\alpha_V(T)$ yields critical exponents α in excellent agreement with those obtained from C_p studies. The available $\alpha_V(T)$ data for 4O.8 [13] are somewhat less detailed but still of considerable value.

Detailed x-ray data have been obtained for smectic scattering in the SmA phase of a few LC's. A by-product of such

*Electronic address: gsiannac@wpi.edu
†Electronic address: cgarland@mit.edu

TABLE I. The N-SmA critical exponent α for the smectic-*A* liquid crystals studied in this work. SmA_d denotes a partial bilayer, and SmA_m denotes a nonpolar monomeric smectic. The α values characterize both the heat capacity and the volume thermal expansion critical behavior and show that these systems lie in an *XY* to tricritical crossover regime. Also given are the stable phases (K=rigid crystal, CrB=plastic crystal B, SmC=smectic-*C*, SmA, N, I=isotropic) and transition temperatures. In the case of K, the melting point on heating is given. Note that the SmC phase is $\overline{8}$S5 and $\overline{10}$S5.

Compound	Smectic type	α [2,7,8,12]	Phases and transition temperatures (K)
8CB	SmA_d	0.31±0.02	K 294.4 SmA 307.0 N 314.0 I
8OCB	SmA_d	0.20±0.03	K 327.6 SmA 340.0 N 353.4 I
$\overline{8}$S5	SmA_m	−0.02±0.02	K 331 SmC 329.2 SmA 336.7 N 359.3 I
$\overline{10}$S5	SmA_m	0.45±0.05	K 339 SmC 337.3 SmA 354.4 N 359.6 I
4O.8	SmA_m	0.13±0.02	K 311.5 CrB 322.3 SmA 336.9 N 352.1 I

high-resolution x-ray studies is good Bragg wave vector $q_0(T)$ data from the $S(q)$ scattering profiles for five LC's: 8CB [16–18], 8OCB [18–20], $\overline{8}$S5 [20–22], $\overline{10}$S5 [23], and 4O.8 [24]. Some of this x-ray work has been associated with recent studies of LC+aerosil systems. In the case of such LC+aerosil studies, it has been shown that $q_0(T)$ for a LC with a low density of dispersed aerosil particles is essentially the same as $q_0(T)$ for the pure bulk LC [17,19,20]. Although the critical behavior of C_p for LC+aerosils evolves with aerosil density [10], the apparent change in $d(T)$ is subtle and only visible close to T_c, where the available data are too sparse to allow a determination of a trend. Thus, utilizing data from both pure LCs and dilute LC+aerosils, the smectic layer thickness $d=2\pi/q_0$, with an average uncertainty of ±0.014 Å, is well known for these five LC's as a function of temperature, yielding the linear thermal expansion coefficient $\alpha_\parallel(T)$ normal to the layer.

Figure 2 shows the $d(T)$ data in the SmA_d phase of 8CB and 8OCB as a plot of $\Delta d=d(T)-d_c$ versus $\Delta T=T-T_c$, where d_c is the layer thickness at the N-SmA critical temperature T_c. Comparable plots in the SmA_m phase of $\overline{8}$S5 and $\overline{10}$S5 are shown in Fig. 3. The linear coefficients $\alpha_\parallel=(1/d)(\partial d/\partial T)_p$ are obtained by differentiation of smooth-curve fits to such $d(T)$ data. The fitting form used is

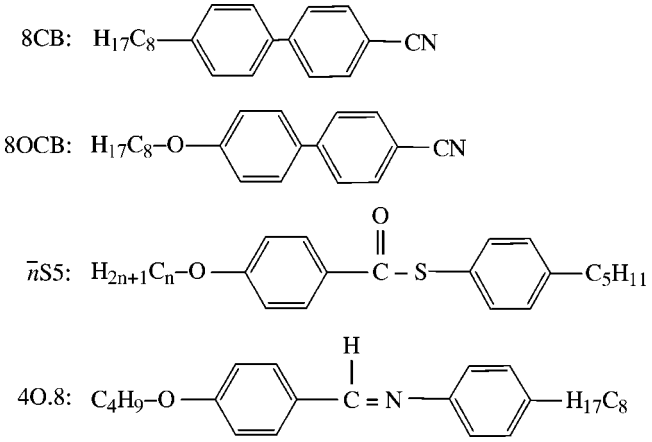

FIG. 1. Structural formulas for liquid crystals referred to in this work.

$$d - d_c \equiv \Delta d = A|\Delta T|^{1-\alpha}(1 + D|\Delta T|^{0.5}) + B(T - T_c), \quad (1)$$

from which one obtains, for $T<T_c$,

$$\alpha_\parallel \simeq \frac{1}{d_c}\left(\frac{\partial d}{\partial T}\right)_p = \frac{-A(1-\alpha)}{d_c}|\Delta T|^{-\alpha}\left[1 + D\left(\frac{1.5-\alpha}{1-\alpha}\right)|\Delta T|^{0.5}\right] + \frac{B}{d_c}. \quad (2)$$

Thus, $\alpha_\parallel=\alpha_\parallel(\text{crit})+\alpha_\parallel(\text{reg})$ where the regular (noncritical) background contribution is a temperature-independent constant:

$$\alpha_\parallel(\text{reg}) = B/d_c. \quad (3)$$

The critical term $\alpha_\parallel(\text{crit})$ has a power-law form with corrections to scaling:

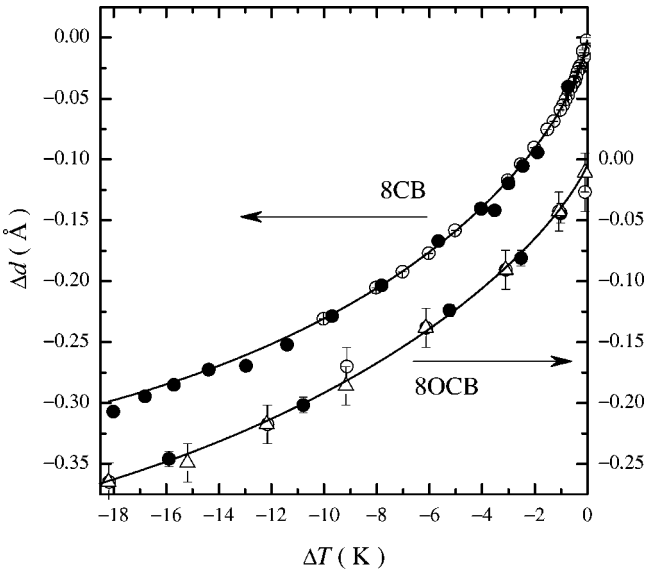

FIG. 2. Dependence of the SmA_d layer thickness d on $T-T_c$, where T_c is the critical T_{NA} transition temperature, for 8CB (LC+sil values: △ from [16] and ● from [17]) and 8OCB (● pure LC, ◯ and LC+sil values [20]). $\Delta d=d-d_c$, where d_c is the value of d at T_c (d_c=31.634 Å for 8CB and d_c=31.720 Å for 8OCB). The solid lines are fits with Eq. (1).

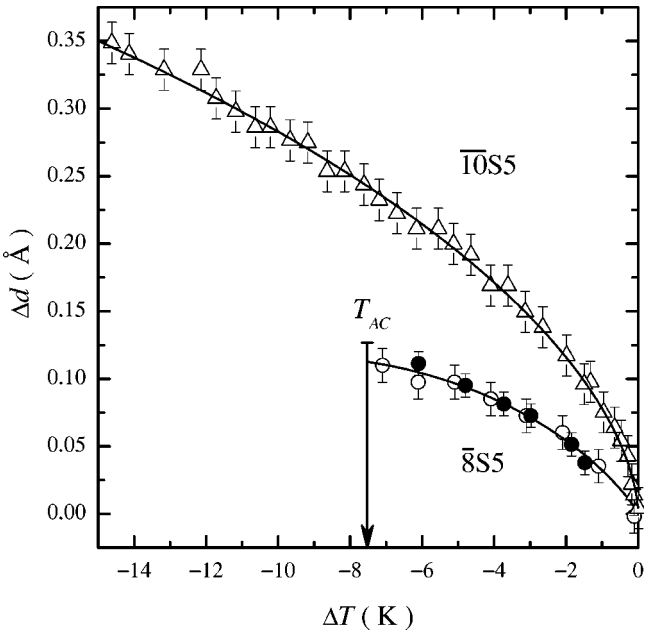

FIG. 3. Dependence of the SmA_m layer thickness d on $T-T_c$, where T_c is the critical T_{NA} transition temperature, for $\overline{8}S5$ (◯ from [20], ● from [22]) and $\overline{10}S5$ (△ from [23]). $\Delta d = d - d_c$, where d_c is the value of d at T_c (d_c=27.890 Å for $\overline{8}S5$ and d_c=30.215 Å for $\overline{10}S5$). The solid lines are fits with Eq. (1). The T_{AC} arrow marks the position of the SmA-SmC transition for $\overline{8}S5$.

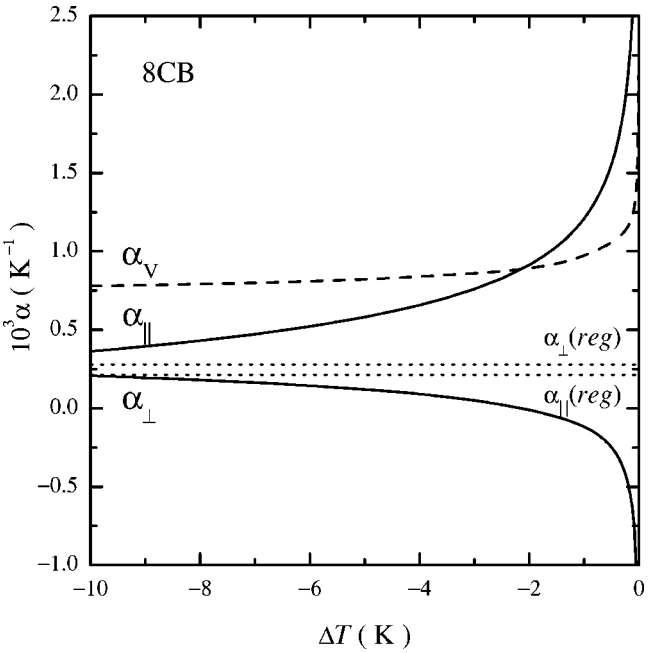

FIG. 4. The linear thermal expansion coefficient $\alpha_\parallel$ normal to the smectic layer (thus parallel to the director) and the in-plane coefficient $\alpha_\perp$ for 8CB. The dashed curve represents the behavior of α_V [7], and the dotted lines show the T-independent values of $\alpha_\parallel$(reg) and $\alpha_\perp$(reg). The value of $1000\alpha_V$(reg) is taken to be 0.77.

$$\alpha_\parallel(\text{crit}) = A_1|\Delta T|^{-\alpha}(1 + D_1|\Delta T|^{0.5}), \tag{4}$$

where $A_1 = -A(1-\alpha)/d_c$ and $D_1 = D(1.5-\alpha)/(1-\alpha)$. The values of the least-squares fit parameters corresponding to the smooth curves given in Figs. 2 and 3 are listed in Table II. The absolute values of d_c and T_c vary slightly from run to run for a given liquid crystal. Neither of these values influence the fit to $\Delta d(\Delta T)$ or the resulting $\alpha_\parallel(\Delta T)$ values, but the best T_c value for each pure bulk LC is given in Table II for convenience and the best d_c values are cited in the legends of Figs. 2 and 3.

The values of the in-plane linear coefficient $\alpha_\perp(\Delta T)$ can be obtained from the fact that in the SmA phase

$$\alpha_V = \alpha_\parallel + 2\alpha_\perp. \tag{5}$$

Thus, combining the x-ray $\alpha_\parallel(\Delta T)$ values with literature $\alpha_V(\Delta T)$ data yields $\alpha_\perp(\Delta T)$. The resulting $\alpha_\parallel(T)$ and $\alpha_\perp(T)$ behaviors, along with $\alpha_V(T)$, are shown in Figs. 4–7 for two SmA_d materials and two SmA_m materials. The critical behavior of 4O.8 will be presented at the end of Sec. III. Also given in Figs. 4–7 as dotted lines are the values of the regular contributions $\alpha_\parallel$(reg) and $\alpha_\perp$(reg). The former is given by Eq. (3), and the latter can be determined from $2\alpha_\perp(\text{reg}) = \alpha_V(\text{reg}) - \alpha_\parallel(\text{reg})$ since α_V(reg) is known from the $V(T)$ data [7,8]. Note the dramatic differences in the magnitude and sign of $\alpha_\parallel$(crit) and $\alpha_\perp(\text{crit}) = \alpha_\perp - \alpha_\perp(\text{reg})$. For both SmA_d LC's 8CB and 8OCB, $\alpha_\parallel$(crit) is positive while $\alpha_\perp$(crit) is negative. The signs of these two terms are reversed for the SmA_m LC's $\overline{8}S5$ and $\overline{10}S5$.

III. CRITICAL BEHAVIOR

The temperature dependences of $\alpha_\parallel$ and $\alpha_\perp$ exhibit obvious critical behavior, as shown by Figs. 4–7. Indeed, differentiation of the least-squares fit to $\Delta d(\Delta T)$ data points yields the form expected for $\alpha_\parallel$ near a second-order critical point.

TABLE II. Fitting parameter values for the least-squares fit of $\Delta d(\Delta T)$ with Eq. (1), where d is in Å units and T is in kelvin.The quantity B was held fixed at the values given in brackets. T_c values are not used in the fit and are given for convenience along with the values of A_1, D_1, and $\alpha_\parallel$(reg) defined in Eqs. (3) and (4).

Material	T_c	α	A	D	B	10^3A_1	D_1	$10^3\alpha_\parallel$(reg)	χ^2_ν
8CB	306.17	0.30±0.05	−0.060±0.008	−0.143±0.015	[0.0067]	1.319	−0.245	0.212	1.055
8OCB	340.09	0.20±0.06	−0.037±0.007	−0.138±0.014	[0.0060]	0.928	−0.224	0.189	1.135
$\overline{8}S5$	336.71	0.05±0.10	0.040±0.015	−0.208±0.028	[−0.003]	−1.356	−0.318	−0.108	1.095
$\overline{10}S5$	353.82	0.42±0.04	0.079±0.006	−0.083±0.013	[−0.006]	−1.526	−0.154	−0.199	1.056

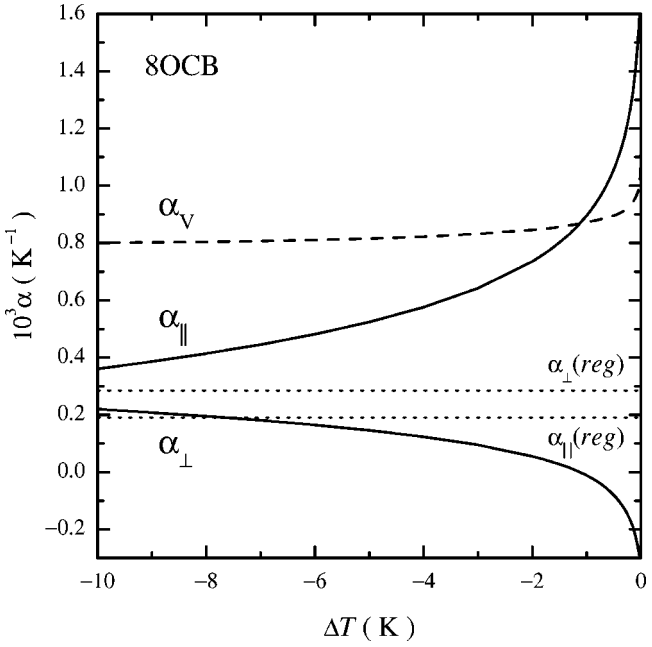

FIG. 5. The linear thermal expansion coefficient $\alpha_\parallel$ normal to the smectic layer (thus parallel to the director) and the in-plane coefficient $\alpha_\perp$ for 8OCB. The dashed curve represents the behavior of α_V [8], and the dotted lines show the T-independent values of $\alpha_\parallel$(reg) and $\alpha_\perp$(reg). The value of $1000\alpha_V$(reg) is taken to be 0.76.

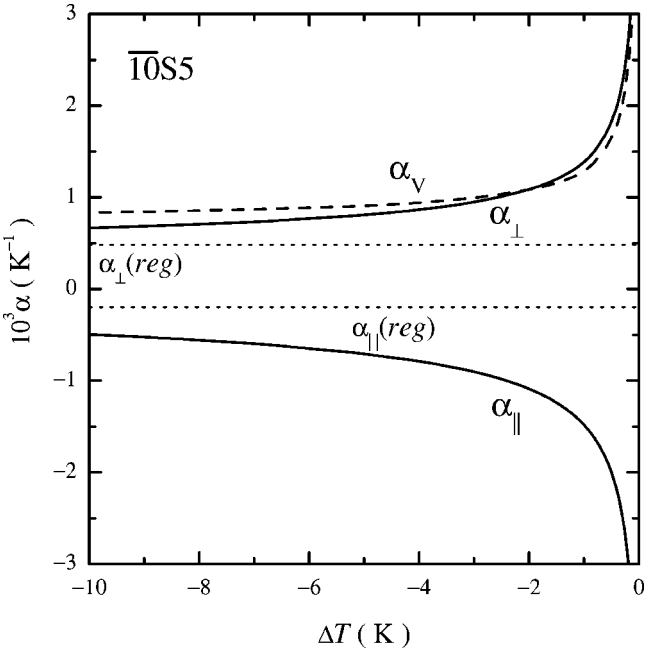

FIG. 7. The linear thermal expansion coefficient $\alpha_\parallel$ normal to the smectic layer (thus parallel to the director) and the in-plane coefficient $\alpha_\perp$ for $\overline{10}$S5. The dashed curve represents the behavior of α_V [7], and the dotted lines show the T-independent values of $\alpha_\parallel$(reg) and $\alpha_\perp$(reg). The value of $1000\alpha_V$(reg) is taken to be 0.77.

The success of Eq. (1) in fitting $d(T)$ implies through Eqs. (2)–(4) that $\alpha_\parallel$ consists of a regular background contribution, which is independent of T, and a power-law critical contribution. The structure of Eq. (4) is exactly the same as that for

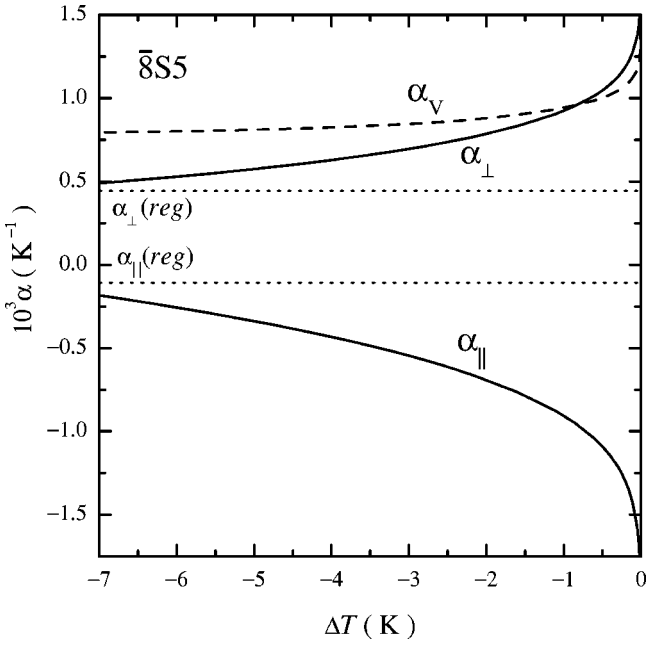

FIG. 6. The linear thermal expansion coefficient $\alpha_\parallel$ normal to the smectic layer (thus parallel to the director) and the in-plane coefficient $\alpha_\perp$ for $\overline{8}$S5. The dashed curve represents the behavior of α_V [8], and the dotted lines show the T-independent values of $\alpha_\parallel$(reg) and $\alpha_\perp$(reg). The value of $1000\alpha_V$(reg) is taken to be 0.78.

the critical heat capacity $C_p - C_p$(reg) [2,10,19] and the critical volume thermal expansion coefficient [7,8]. Furthermore, the critical exponents α given in Table II and those given in Table I, which were obtained from C_p(crit) and α_V(crit), are in excellent agreement. This agreement between the independently determined exponents α that characterize the critical behavior of $\alpha_\parallel$ and α_V is essentially required if a power-law form is valid for either quantity. Equation (5) is a completely general expression, and it could not be satisfied if α_V, $\alpha_\parallel$, and $\alpha_\perp$ had different critical singularities.

It should be noted that we have fixed the fit parameter B in order to prevent strong coupling between the terms $B(T - T_c)$ and $AD|\Delta T|^{(1.5-\alpha)}$ in Eq. (1) from causing unstable least-squares minimization. However, this does not have a great influence on the least-squares value of the critical exponent α. Stepping B values through a series of physically plausible values changes α by about ±0.05 (95% confidence limit) except for $\overline{8}$S5 where it is ±0.1. Furthermore, $\alpha_\perp$(reg) must have a physically reasonable value. This consideration puts another constraint on possible choices for the value of B.

There is another way to show that the critical behavior of $\alpha_\parallel$ is the same as that for α_V which does not depend on using power-law fits to either quantity. The generalized Pippard equations [25,26] are thermodynamic expressions that have been shown to hold for the thermal and elastic properties near second-order phase transitions. The significant equations for the present purposes are

$$\alpha_V = s_V\left(\frac{C_p}{VT}\right) - g_V, \tag{6}$$

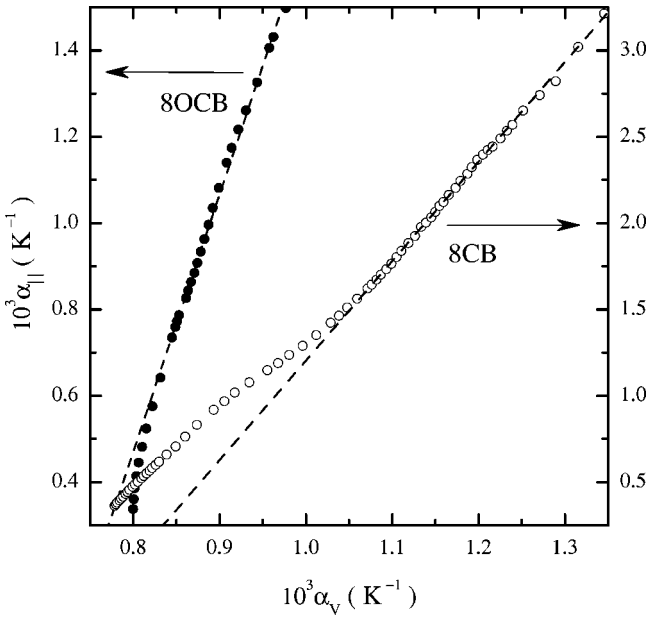

FIG. 8. Pippard plot of $\alpha_{\|}$ versus α_V for 8CB (◯) and 8OCB (●). The slope of the linear portion representing data close to T_c (dashed line) gives the ratio $(dT_c/dp_{\|})/(dT_c/dp)$.

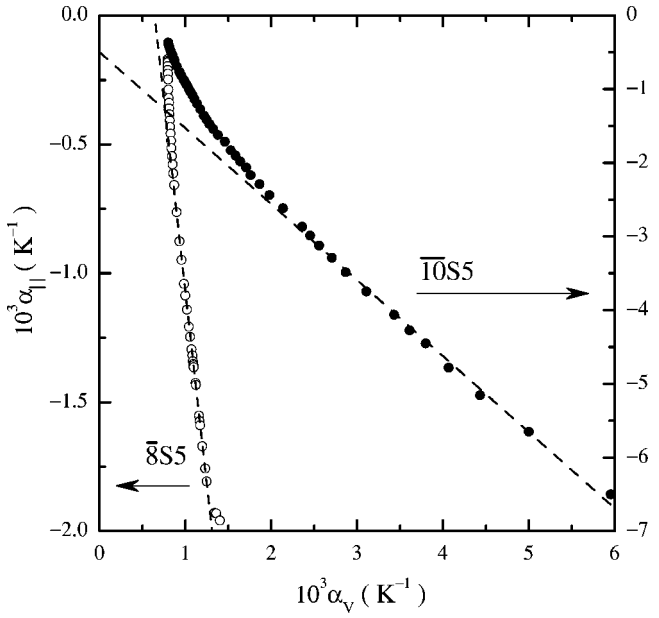

FIG. 9. Pippard plot of $\alpha_{\|}$ versus α_V for $\overline{8}$S5 (◯) and $\overline{10}$S5 (●). The slope of the linear portion representing data close to T_c (dashed line) gives the ratio $(dT_c/dp_{\|})/(dT_c/dp)$.

$$\alpha_{\|} = s_{\|}\left(\frac{C_p}{VT}\right) - g_{\|}, \tag{7}$$

$$\alpha_{\perp} = s_{\perp}\left(\frac{C_p}{VT}\right) - g_{\perp}, \tag{8}$$

where all g_i are effectively constants [27]. The quantity $s_V \equiv dT_c/dp$ is the hydrostatic pressure dependence of T_c, while $s_{\|} \equiv -(dT_c/dX_{\|})_{X_{\perp}} = dT_c/dp_{\|}$ and $s_{\perp} \equiv -(dT_c/dX_{\perp})_{X_{\|}} = dT_c/dp_{\perp}$ give the variation of T_c with a uniaxial pressure (X_i is the uniaxial stress and $p_i = -X_i$ is the definition of a uniaxial pressure).

It follows from Eqs. (6) and (7) that

$$\alpha_{\|} = \left(\frac{dT_c/dp_{\|}}{dT_c/dp}\right)\alpha_V - c_{\|}, \tag{9}$$

where $c_{\|}$ is $(s_{\|}/s_V)g_V - g_{\|}$. This equation can be tested by plotting the x-ray $\alpha_{\|}$ values versus dilatometric α_V values, as shown in Figs. 8 and 9. The points that appear in these figures are not experimental data points but are generated at a series of closely spaced $|\Delta T|$ values by interpolation in the $\alpha_V(\Delta T)$ data set [7,8] and from our $\alpha_{\|}(\Delta T)$ curves. The emphasis in viewing these figures should be on the linear region corresponding to small $|\Delta T|$ values, which is of course the region where α_V is large. In this region, any variation in the"constant" $c_{\|}$ with $|\Delta T|$ [27] will be small compared to the rapid variation with $|\Delta T|$ in $\alpha_{\|}$ and α_V values. Thus the ratio $(dT_c/dp_{\|})/(dT_c/dp)$ in Eq. (9) has been taken to be the slope of the dashed straight lines fitting the behavior close to T_c. The important conclusion from the existence of a linear Pippard plot over a range of small $|\Delta T|$ values is that $\alpha_{\|}$ has the same critical singularity as α_V. Although there is an equation for $\alpha_{\perp}$ analogous to Eq. (9), this is not an independent equation since $s_V = s_{\|} + 2s_{\perp}$ by definition and $\alpha_V = \alpha_{\|} + 2\alpha_{\perp}$ has been used to generate the $\alpha_{\perp}$ values from $\alpha_{\|}$ and α_V values. Thus it follows trivially that $\alpha_{\perp}$ must exhibit the same criticality.

The values of dT_c/dp are known from high-pressure experiments on many LC's. Since Figs. 8 and 9 show that Eq. (9) holds very well for small $|\Delta T|$, the slopes of those plots allow us to find $dT_c/dp_{\|}$. The values of dT_c/dp, $dT_c/dp_{\|}$, and $dT_c/dp_{\perp}$ are given in Table III. It is clear from Eqs. (7) and (8) and Table III that the different magnitudes and signs for the critical contributions to $\alpha_{\|}$ and $\alpha_{\perp}$ are due to differences in the variation of T_c with uniaxial pressure normal to the smectic layer ($p_{\|}$) and in the plane of the layer ($p_{\perp}$). Since the pattern of signs is the same for 8CB and 8OCB and opposite signs hold for $\overline{8}$S5 and $\overline{10}$S5, one might be tempted to think that all SmA_d LC's are like 8CB and all SmA_m LC's are like $\overline{n}$S5. This speculation may be true with regard to signs, but consideration of data for 4O.8, another SmA_m material, shows a dramatic difference in the magnitude of $dT_c/dp_{\|}$ for $\overline{n}$S5 and nO.m LC's.

TABLE III. Values of dT_c/dp and the quantities $s_{\|} \equiv dT_c/dp_{\|}$ and $s_{\perp} \equiv dT_c/dp_{\perp}$ obtained from the slopes of Pippard plots for several liquid crystals. In all cases, the units are K $kbar^{-1}$. The references giving the experimental values of dT_c/dp are cited.

Material	dT_c/dp	$dT_c/dp_{\|}$	$dT_c/dp_{\perp}$
8CB	22.85 [28,29]	131.7	−54.4
8OCB	17.36 [30,31]	103.5	−43.1
$\overline{8}$S5	20.20 [32]	−60.38	40.29
$\overline{10}$S5	18.35 [33]	−18.94	18.64
4O.8	20.40 [13]	0	10.2

X-ray data obtained in the SmA phase of 4O.8 [24] show that the layer thickness d is independent of T over the entire 15-K-wide SmA range. Thus, $\alpha_{\|}=0$ and $\alpha_{\perp}=\alpha_V/2$ for 4O.8. This striking result $\alpha_{\|}=0$ in the SmA phase is not some accidental value for 4O.8 but holds for many nO.m LC's such as 4O.7 [34], 5O.6 and 5O.7 [35], and 5O.8 and 5O.10 [36]. Note that the critical behavior of C_p and α_V for 4O.8 [5,13,37] and other nO.m compounds [38,39] fits into the same pattern as the $\overline{n}$S5 compounds; see Ref. [2]. Since C_p exhibits a critical singularity for 4O.8 but $\alpha_{\|}$ does not, Eq. (7) requires that $dT_c/dp_{\|}=0$. Further support for the idea that nO.m materials differ from other SmA materials is provided by the fact that $\alpha_V(\Delta T)$ near the $T_c(p)$ critical line for the N-SmA transition is independent of hydrostatic pressure for 4O.8 [13] and 8O.m with $m=5$, 6, 7, 9 [39]. Equation (6) then implies that C_p(crit) must be a function of $(T-T_c)$ only and independent of p at least over a moderate pressure range from 1 to 1000 bars. This differs greatly from the strong pressure dependence of C_p(crit) observed in other LC's such as 8CB and 8OCB [40,41].

IV. DISCUSSION

Determination of $\alpha_{\|}$(crit) and $\alpha_{\perp}$(crit) provides some insight into the stability of the SmA phase to stresses and is thus linked to the tendency for SmA on cooling to form SmC, CrB, or even reentrant nematic N_r. We shall address here the plausible reasons that $\alpha_{\|}$(crit) is positive for 8CB and 8OCB (SmA$_d$ materials with biphenyl cores) but negative for $\overline{8}$S5 and $\overline{10}$S5 (SmA$_m$ materials with a flexible -C(O)-S-link between the core phenyl rings).

For the LC's nCB and nOCB, permeation along the director is the dominant mechanism for the growth of SmA$_d$ order below the transition. During this process, there is only a minor change in the lateral alignment of neighboring LC molecules and the ordering primarily involves better interdigitation of rodike molecules to form a "dimerlike" partial bilayer [42]. Thus, one can understand why increasing the uniaxial pressure $p_{\|}$ would push the LC rods into a better layer structure and stabilize the SmA$_d$ phase. This implies that $dT_c/dp_{\|}>0$, and the Pippard equation (7) then predicts $\alpha_{\|}$(crit)>0. In the same context, increasing the in-plane pressure $p_{\perp}$ will force the bulky "dimer" cores to shift up or down away from the center of the SmA$_d$ layer in order to allow better in-plane packing. Thus, an increase in $p_{\perp}$ destabilizes the SmA$_d$ phase, which implies that $dT_c/dp_{\perp}<0$ and leads via Eq. (8) to $\alpha_{\perp}$(crit)<0 (see Fig. 1).

For the liquid crystals $\overline{n}$S5, the flexible -C(O)-S-link in the core means that the molecule is slightly bent near the center [32] and the two aromatic rings are twisted quite a bit relative to each other. As the SmA$_m$ order increases on cooling below the transition, there is an improvement in the lateral alignment of these bent rods, and permeation along the director plays an important but smaller role. For such LC's, increasing the in-plane pressure $p_{\perp}$ may tend to partially straighten the molecules and will definitely improve the "nesting" of such molecules. This improves the layer structure and stabilizes the SmA$_m$ phase, which implies that

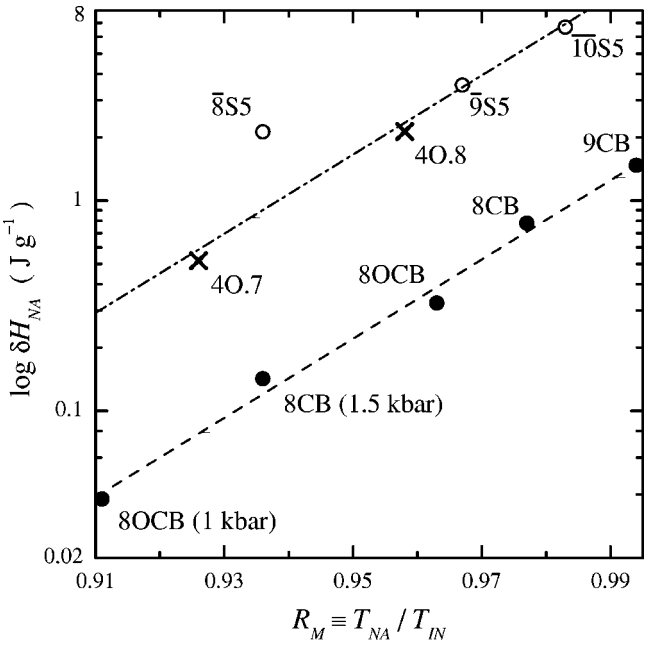

FIG. 10. The integrated N-SmA enthalpy δH_{NA} versus the McMillan ratio R_M for a variety of smectic liquid crystals. The dashed line gives the empirical trend for these SmA$_d$ LC's, and the dashed-dot line represents δH_{NA} values that are arbitrarily taken to be 7.5 times larger.

$dT_c/dp_{\perp}>0$ and therefore $\alpha_{\perp}$(crit)>0. An increase in $p_{\|}$ will tend to buckle the molecule (increase the bend at the core link), and this makes these molecules pack less well in the SmA$_m$ layer. Thus, SmA$_m$ is destabilized and $dT_c/dp_{\|}<0$, leading to $\alpha_{\|}$(crit)<0.

Support for the above ideas is provided by Fig. 10, which shows the variation of the integrated enthalpy δH_{NA} with the McMillan parameter R_M [43–45]. Note that δH_{NA} for the cyanobiphenyl SmA$_d$ compounds is $\sim$7.5 times smaller than that for $\overline{n}$S5 SmA$_m$ compounds with the same R_M value. These low δH_{NA} values for SmA$_d$ compounds are due to the fact that most of the N-SmA enthalpy in any LC is due to changes in the van der Waals term related to changes in the lateral alignment of neighboring molecules. In SmA$_d$ compounds, there is not much enthalpy associated with sliding molecular pairs (loose "dimers") up and down along the director. Another source of support for the above ideas is the variation with R_M of the enhancement δS of the nematic orientational order when a LC system goes from the nematic phase into the SmA phase. In general, δS decreases as R_M decreases. It is also observed that the magnitude of δS is appreciably smaller for SmA$_d$ than for SmA$_m$ compounds for a given R_M [46]. This indicates that the orientational order in the nematic phase just above T_{NA} is better for SmA$_d$ than for SmA$_m$ materials, which means the axis for permeation is "easier," with less change occurring in the lateral packing on cooling into the SmA$_d$ phase.

It is necessary to comment now on the behavior of 4O.8 and other nO.m compounds, where $\alpha_{\|}$(crit)$=0$. The reason that this is different from the behavior of $\overline{n}$S5 LC's can be found in the molecular structure. 4O.8 has a rigid -C(H)=N-link between the rings in the core. Thus the 4O.8 mol-

ecule is relatively stiff and difficult to bend. Both 4O.8 and 8S5 are monomeric smectics [47], but the *n*S5 compounds with their bent shape exhibit a SmC phase when SmA_m is cooled. In contrast, 4O.8 exhibits a plastic crystal CrB phase [48] when SmA_m is cooled, and the "layer" spacing in CrB is only 1% greater than the SmA_m d value. Most nO.m compounds show that same phase sequence [39,49]. Thus increasing $p_\parallel$ for 4O.8 has little or no effect: there is no dominant permeation mechanism, so $p_\parallel$ will not stabilize the SmA_m phase; there is no bend or buckling tendency, so $p_\parallel$ will not destabilize SmA_m. Thus it is not surprising that $dT_c/dp_\parallel=0$ for 4O.8, which is implied by the observed $\alpha_\parallel=0$. The application of an in-plane pressure $p_\perp$ to 4O.8 should somewhat improve the lining up of molecules in the SmA_m phase and thus stabilize this phase. Therefore, one would expect $dT_c/dp_\perp>0$, which is consistent with $\alpha_\perp>0$. Note, however, that $dT_c/dp_\perp$ is small, presumably due to the similar packing in the SmA_m and CrB phases, which implies that the molecules are already fairly well aligned in the SmA_m phase at ambient (1-bar) pressure.

Future work on the linear expansion coefficients $\alpha_\parallel$ and $\alpha_\perp$ in the SmA phase would be of interest. Such studies would be easy for 9CB (critical exponent $\alpha=0.50$), where $V(T)$ and dT_c/dp data are already available [14,50] and only x-ray data are lacking. In the case of 4O.7 (critical $\alpha=-0.007$) and 9S5 (critical $\alpha=0.22$), good x-ray data on the smectic phaselayer spacing $d(T)$ are available [23,34], but data on both $V(T)$ and dT_c/dp are needed. It would also be especially interesting to study frustrated smectics like DB_8ONO_2 (octyloxyphenylnitrobenzoyloxy benzoate) and T7 (heptyloxybenzoyloxy cyanostilbene), where there are rigid three-ring cores and huge N ranges. It is observed in these materials that the critical behavior of all properties near T_{NA} is close to the ideal 3D XY limit [6].

ACKNOWLEDGMENTS

The authors wish to thank P. Clegg, W. de Jeu, R. Leheny, B. Ocko, C. Safinya, J. Thoen, and especially A. Zywocinski for providing detailed unpublished data as well as useful commentary. We also thank J. Nibler for the Gaussian calculation of molecular lengths for 4O.8 and 8S5. This work was supported at WPI by the NSF under CAREER Award No. DMR-0092786.

[1] P. G. de Gennes and J. Prost, *The Physics of Liquid Crystals* 2nd ed. (Oxford University Press, Oxford, 1993).
[2] C. W. Garland and G. Nounesis, Phys. Rev. E **49**, 2964 (1994) and references cited therein.
[3] J. Thoen, Int. J. Mod. Phys. B **9**, 2157 (1995); J. Thoen, H. Marynissen, and W. VanDael, Phys. Rev. A **26**, 2886 (1982).
[4] J. Als-Nielsen *et al.*, Phys. Rev. B **22**, 312 (1980).
[5] K. J. Stine and C. W. Garland, Phys. Rev. A **39**, 3148 (1989).
[6] C. W. Garland, G. Nounesis, M. J. Young, and R. J. Birgeneau, Phys. Rev. E **47**, 1918 (1993).
[7] A. Zywocinski and S. A. Wieczorek, J. Phys. Chem. B **101**, 6970 (1997).
[8] A. Zywocinski, S. A. Wieczorek, and J. Stecki, Phys. Rev. A **36**, 1901 (1987).
[9] S. Shibahara *et al.*, J. Phys. Soc. Jpn. **71**, 802 (2002); P. Martinoty, P. Sonntag, L. Benguigui, and D. Collin, Phys. Rev. Lett. **73**, 2079 (1994); F. Beaubois *et al.*, Phys. Rev. E **56**, 5566 (1997); see also references cited in [2].
[10] G. S. Iannacchione *et al.*, Phys. Rev. E **67**, 011709 (2003).
[11] The notation SmA_m is used for nonpolar "monomeric" LC's with alkyl or alkoxy chains at both ends, where $d\cong 0.9L-L$, with L being the extended length of a single LC molecule. For partial bilayer SmA_d materials, d is typically $1.35L-1.5L$.
[12] M. Marinelli, F. Mercuri, U. Zammit, and F. Scudieri, Phys. Rev. E **53**, 701 (1996).
[13] S. M. Stishov, S. N. Nefedov, and A. N. Zisman, JETP Lett. **36**, 348 (1982); S. N. Nefedov, A. N. Zisman, and S. M. Stishov, Sov. Phys. JETP **59**, 71 (1984).
[14] V. N. Raja, S. Krishna Prasad, D. S. Shankar Rao, and S. Chandrasekhar, Liq. Cryst. **12**, 239 (1992).
[15] A. Zywocinski, J. Phys. Chem. B **106**, 11 711 (2002); G. A. Oweimreen, *ibid.* **106**, 11 708 (2002).
[16] D. Liang, M. Borthwick, and R. L. Leheny, J. Phys.: Condens. Matter **16**, S1989 (2004); R. L. Leheny (private communication).
[17] R. L. Leheny *et al.*, Phys. Rev. E **67**, 011708 (2003); see also S. Park, Ph.D. dissertation, MIT, 2001 (unpublished).
[18] J. Przedmojski *et al.*, Phase Transit. A **56**, 119 (1996).
[19] P. S. Clegg *et al.*, Phys. Rev. E **67**, 021703 (2003).
[20] P. S. Clegg (private communication).
[21] P. S. Clegg *et al.*, Phys. Rev. E **68**, 031706 (2003).
[22] C. Safinya (private communication).
[23] B. M. Ocko, R. J. Birgeneau, and J. D. Litster, Z. Phys. B: Condens. Matter **62**, 487 (1986).
[24] W. H. deJeu (private communication); see also A. Fera *et al.*, Phys. Rev. E **60**, R5033 (1999).
[25] C. W. Garland, J. Chem. Phys. **41**, 1005 (1964); V. Janovec, *ibid.* **45**, 1874 (1966).
[26] J. P. Bachheimer and G. Dolino, Ferroelectrics **25**, 423 (1980); see also H. Sakashita, N. Ohama, and A. Okazaki, Phase Transitions **28**, 99 (1990) for a material with two critical linear expansion coefficients of opposite sign.
[27] The quantities g_i are rigorously constant only if the original cylindrical approximation of Pippard is valid. However, even in less idealized situations, these quantities are slowly varying functions of $|T-T_c|$ that are effectively constant for a range of small to moderate $|T-T_c|$ values, whereas C_p and the various thermal expansion coefficients α_i are large and rapidly varying (divergent). Far from T_c, i.e., for large $|T-T_c|$, Pippard plots of α_i vs C_p may exhibit nonlinearity due to mild variations in g_i. See M. J. Buckingham and W. M. Fairbank, *Progress in Low Temperature Physics* (North-Holland, Amsterdam, 1961), Vol. 3, Chap. 3.
[28] G. B. Kasting, C. W. Garland, and K. J. Lushington, J. Phys.

(Paris) **41**, 879 (1980).
[29] P. E. Cladis, R. K. Bogardus, and D. Aadsen, Phys. Rev. A **18**, 2292 (1978); S. Urban, T. Bruckert, and A. Wurflinger, Z. Naturforsch., A: Phys. Sci. **49**, 552 (1994); P. Markwich, S. Urban, and A. Wurflinger, *ibid.* **54**, 275 (1999).
[30] G. B. Kasting, K. J. Lushington, and C. W. Garland, Phys. Rev. B **22**, 321 (1980).
[31] P. E. Cladis, R. K. Bogardus, W. B. Daniels, and G. N. Taylor, Phys. Rev. Lett. **39**, 720 (1997).
[32] P. E. Cladis *et al.*, Mol. Cryst. Liq. Cryst. Lett. **49**, 279 (1979).
[33] S. L. Randzio, J. Therm. Anal. **38**, 1989 (1992).
[34] B. M. Ocko, A. R. Kortan, R. J. Birgeneau, and J. Goodby, J. Phys. (Paris) **45**, 113 (1984).
[35] P. R. Alapati, D. M. Potukuchi, N. V. S. Rao, and V. G. K. M. Pisipati, Liq. Cryst. **3**, 1461 (1988).
[36] R. Caciuffo, S. Melone, and G. Torquati, Nuovo Cimento D **7**, 421 (1986).
[37] H. Haga and C. W. Garland, Phys. Rev. E **56**, 3044 (1997).
[38] C. W. Garland *et al.*, Phys. Rev. A **27**, 3234 (1983).
[39] C. R. C. Prabhu and V. G. K. M. Pisipati, Cryst. Res. Technol. **37**, 269 (2002) and references cited therein.
[40] G. B. Kasting, C. W. Garland, and K. L. Lushington, J. Phys. (Paris) **41**, 879 (1980).
[41] G. B. Kasting, K. J. Lushington, and C. W. Garland, Phys. Rev. B **22**, 321 (1980).
[42] A. J. Leadbetter *et al.*, J. Phys. (Paris) **40**, 375 (1979).
[43] E. Bloemen and C. W. Garland, J. Phys. (Paris) **42**, 1299 (1981).
[44] D. Brisbin, R. De Hoff, T. E. Lockhart, and D. L. Johnson, Phys. Rev. Lett. **43**, 1171 (1979).
[45] J. Thoen (private communication).
[46] Values of δS at the N-SmA transition have been determined from both birefringence Δn and NMR quadrupolar splitting $\delta\nu$. Unfortunately, high-resolution and precise data for δS are sparse, but the difference between SmA_m and SmA_d compounds is qualitatively clear. See N. Boden *et al.*, Mol. Phys. **42**, 565 (1981); D. Catalano *et al.*, Liq. Cryst. **2**, 345 (1987); B. M. Fung *et al.*, *ibid.* **4**, 1495 (1993); R. Y. Dong, Phys. Rev. E **60**, 5631 (1999) for NMR data. See N. R. Chen, S. K. Hark, and J. Ho, Phys. Rev. A **24**, 2843 (1981); E. F. Gramsbergen and W. H. de Jeu, J. Chem. Soc., Faraday Trans. 2 **84**, 1015 (1988); J. Ho (private communication) for birefringence data.
[47] For 8S5 at a temperature in the center of the SmA_m phase, the layer spacing $d=27.97\pm0.2$ Å and a Gaussian quantum-mechanical calculation gives 29.0 ± 0.1 Å for the length L of a single molecule. Thus $d/L=0.965$. For 4O.8, $d=28.2\pm0.2$ Å for all T in the SmA_m range, and the Gaussian-calculated value of L is 27.3 ± 0.1 Å. Thus $d/L=1.033$ for 4O.8.
[48] D. E. Moncton and R. Pindak, Phys. Rev. Lett. **43**, 701 (1979); P. S. Pershan, G. Aeppli, J. D. Litster, and R. J. Birgeneau, Mol. Cryst. Liq. Cryst. **67**, 2051 (1981).
[49] V. G. K. M. Pisipati and S. B. Rananavare, Liq. Cryst. **13**, 757 (1993).
[50] T. Shirakawa, Y. Kikuchi, and T. Seimiya, Thermochim. Acta **197**, 399 (1992).